Scientific Research Publishing

American Journal of Plant Sciences, 2023, 14, 41-63
https://www.scirp.org/journal/ajps
ISSN Online: 2158-2750
ISSN Print: 2158-2742

Impact of Different Light Characteristics on the Growth and Lipid Content of Diatom *Phaeodactylum tricornutum* Transconjugant Strains

Nikunj Sharma, Elisa Ines Fantino, Fatima Awwad, Natacha Mérindol, Arun Augustine, Fatma Meddeb, Isabel Desgagné-Penix

Department of Chemistry, Biochemistry and Physics, Université du Québec à Trois-Rivières, Trois-Rivières, Québec, Canada
Email: Nikunj.Sharma@uqtr.ca

How to cite this paper: Sharma, N., Fantino, E.I., Awwad, F., Mérindol, N., Augustine, A., Meddeb, F. and Desgagné-Penix, I. (2023) Impact of Different Light Characteristics on the Growth and Lipid Content of Diatom *Phaeodactylum tricornutum* Transconjugant Strains. *American Journal of Plant Sciences*, **14**, 41-63.
https://doi.org/10.4236/ajps.2023.141004

Received: November 22, 2022
Accepted: January 17, 2023
Published: January 20, 2023

Abstract

Light regulates important metabolic processes in microalgal cells, which can further impact the metabolism and the accumulation of biomolecules such as lipids, carbohydrates, and proteins. Different characteristics of light have been studied on various strains of the model diatom *Phaeodactylum tricornutum*, but not on transconjugant cells and information on wild-type strains is still limited. Therefore, we studied the impact of different light characteristics such as spectral quality, light intensity and light shift on the growth, and the composition in lipids and fatty acids of *P. tricornutum* cells to provide a comprehensive context for future applications. Initially, we tested the impact of spectral quality and light intensity on *P. tricornutum* transformed with an episomal vector (*Pt*ev), harboring the resistance gene S*h ble*. Results indicated that *Pt*ev cells accumulated more biomass and overall lipids in spectral quality Red 1 (R1: 34% > 600 nm > 66%) more effectively as compared to Red 2 (R2: 8% > 600 nm > 92%). It was also detected that cell granularity was higher in R1 as compared to R2. Furthermore, by testing two light intensities 65 µmol·m^{-2}·s^{-1} and 145 µmol·m^{-2}·s^{-1} light, it was observed that 145 µmol·m^{-2}·s^{-1} led to an increase in growth trend, total biomass and lipid content. Combining spectral qualities and light intensities, we show that the lipid accumulation raised by 2.8-fold. Studying the light intensity and spectral quality allowed us to optimize the light conditions to R1 spectral quality and light intensity 145 µmol·m^{-2}·s^{-1}. These initial results showed that red light R1 at 145 µmol·m^{-2}·s^{-1} was the best condition for biomass and total lipids accumulation in *Pt*ev cells. Next, we further combined these two-light optimizations with a third light characteristics, *i.e.* light shift,

where the cultures were shifted during the early stationary phase to a different light environment. We studied Red light shift (Rs) to investigate how light condition variations impacted *P. tricornutum* transconjugants *Pt*ev and with an episomal vector containing the reporter gene YFP (*Pt*YFP). We observed that Rs induced growth and fatty acid eicosapentaenoic acid (EPA) in *Pt*ev as compared to *Pt*YFP. Altogether, the study shows that red light shift of R1 at 145 $\mu mol \cdot m^{-2} \cdot s^{-1}$ promoted biomass and total lipids accumulation in *Pt*ev and *Pt*YFP cells. The study provides a comprehensive approach to using different light characteristics with the aim to optimize growth and lipids, as well as to fatty acid production.

Keywords

Phaeodactylum tricornutum, Light Condition, Episomal Vector, Diatoms, Fatty Acids, Biomass

1. Introduction

Currently, there is a growing concern about the need of renewable feedstock for human fulfilment and the consequences of overconsumption by the ever-growing human population. Our society would highly benefit from including the principles of bioeconomy, such as using more renewable biomass and utilizing/recycling by-products, instead of non-renewable feedstock for non-essential uses [1]. Microalgae and diatoms hold a big potential to contribute to solving issues related to the lack of renewable feedstock because of their possible usage in fossil fuel-based technologies [2] [3] [4] [5]. Moreover, the use of the diatom *Phaeodactylum tricornutum* species to produce a variety of industrially important bioproducts (*e.g.* fatty acids, pigments, vitamins), is gaining interest [6]. For example, fatty acid derivatives, such as hydroxy fatty acids, fatty alcohols, fatty acid methyl/ethyl esters, and fatty alka(e)nes, have a wide range of industrial applications including bioplastics, cosmetics, pharmaceutics, lubricants, and fuels [7].

Adaptability, maintenance, and regulation of biochemical and physiochemical processes under high stress conditions are key features of diatoms, which are exploited for bio-products production for sustainable economy [8]. These characteristics give diatoms the plasticity to respond and survive in the changing ecosystem and to utilize the resource most efficiently [8] [9] [10]. Diatoms have the potential to adapt to different conditions such as variations in light intensity, spectral quality and light shift [11] [12] [13]. It is well established that precise light condition has a significant and strong impact on the overall functioning of microalgae photosystem and nutrient cycle. For example, blue light controls the onset of cell division, while shifting the culture from red to blue light increases the production of proteins [10]. Spectral quality also influences light signaling pathways [10] [12] [14] [15] [16] [17] [18]. Several studies have reported on the

impact of different spectral light qualities on *P. tricornutum* growth, biomass, lipids and pigment accumulation [19] [20] [21]. It was observed that, red and blue lights have an impact on accumulation of sterols [20], lipids [22] and pigments [23]. The total amount of sterols was lowest in blue light and sterol glycosylation was affected with a 100-fold decrease in steryl glycosides under blue light and a 100-fold decrease in acylated steryl glycosides under red light [20]. In addition to the spectral quality, and variations in light intensity affects the growth and metabolites production by manipulating biological processes such as membranes remodeling, polyunsaturated fatty acids (PUFA) biosynthesis, rerouting, light-harvesting or photo-protection activity in *P. tricornutum* [23] [24].

More recently, metabolic engineering has been used to investigate the potential of diatoms for industrial uses such as increasing the total biomass or metabolites production. For example, the biolistic transformation of *P. tricornutum* has been used to produce omega fatty acids, betulin and its precursors [25] [26]. Also, studies have shown that overexpression of reporter genes such as GFP and YFP impacted the growth and biomass of *P. tricornutum* and *Rhodobacter sphaeroaides* [27] [28]. Furthermore, overexpression of a putative plastidial pyruvate transporter has been used to increase biomass, lipid content, and growth [29]. For the production of proteins or metabolites of interest, metabolic engineering researchers exploit the potential of bacteria and yeasts, however these platforms do not always support the assembly of complex plant-derived metabolic pathways. Microalgae cells possess several advantages over other microorganisms; 1) unlike prokaryotic bacteria, microalgae are able to perform the post-translational modifications of recombinant proteins necessary to the native eukaryotic organism, 2) as is the case in plants, recombinant protein expression in microalgae can be done through the nuclear, mitochondrial or chloroplastic genomes. The latter is well established and allows one to successfully bypass nuclear regulation mechanisms, 3) microalgae biomass doubles in size every 48 hours allowing rapid large-scale production, 4) autotrophic or heterotrophic growth conditions can be used, 5) cultivation in photobioreactors insure control of growth conditions and prevents the possible escape of transgenes into the wild. Thus, microalgae such as diatoms represent an ideal platform to support the production of complex plant metabolites [30]. Nuclear transformation offers the advantages of post-translational modifications of recombinant proteins, the possibility of protein targeting and flexibility in regulatory expression (native or heterologous promoters and untranslated regions). However, the main disadvantage of nuclear transformation is the low expression levels of the genes of interest due to silencing and positions effects (random integration). The chloroplastic gene transformation offers higher levels of transgenic protein accumulation but is comprise in the chloroplast, lacks post-translational modifications, and is limited in regulatory tools. Both, nuclear and chloroplastic transformation are also limited in the size of the transgenes to be inserted. Recently, Slattery *et al.* have used the robust episomal conjugative system to edit urease gene with 60% efficiency and stably transform eight genes involved in vanillin synthesis for 4 months with no rear-

rangement [31]. To this date, no study has reported on the impact of the episomal vector and the presence of reporter gene on *P. tricornutum* growth and metabolism. Therefore, we have used the episomal based transformation to insert the Yellow Fluorescent Protein (YFP) as reporter gene to analyze its impact on growth, lipid, and fatty acid profile.

In the actual context, *P. tricornutum* holds great promise for the light-driven bioproduction of biofuels and high-value, industrially relevant biochemicals [6]. They are the primary food and energy sources in many aquatic food systems and play an important ecological role in global carbon and silicon cycling. In this study, we aim to provide a comprehensive strategy to study light-based experiments on bioengineered *P. tricornutum* to get a view of light intensity, light shift and spectral quality impact on biomass, lipid accumulation and fatty acid composition. Furthermore, we provide a proof of concept to acknowledge the importance of culture conditions on diatoms-based compounds production both in *P. tricornutum* containing the resistant gene *Sh ble* in the episomal vector (*Pt*ev) and *P. tricornutum* YFP transconjugants harboring genes encoding YFP fluorescent proteins (*Pt*YFP). We also analyzed the effect of light on YFP accumulation by studying YFP fluorescence levels and the lipid accumulation and fatty acid composition of *P. tricornutum*.

2. Methodology

2.1. Growth and Culture Conditions

Axenic *P. tricornutum* Bohlin, (Culture Collection of Algae and Protozoa CCAP 1055/1), was kindly provided by Prof. Bogumil Karas from Western University, Canada. Cultures were maintained in L1 media. Experiments for growth curve were done in 250 mL flask with 50 mL L1 media with an equal inoculum size of 0.2 OD at absorbance 680 nm (OD_{680nm}). *P. tricornutum* cells were grown and maintained in L1 media without silica at pH 8 (Artificial Sea Water) in a growth chamber at 18˚C ± 1.5˚C with cool white light, as standard condition, for 16:8h light/dark photoperiod of cycles and shaking at 120 rpm.

2.2. Transconjugant Strains Generation and Selection

Recombinant plasmid named here *Pt*YFP consist in the pPtGE30 plasmid (*Pt*ev) [31] carrying genes of interest fused to yellow fluorescent protein (YFP) in N-terminal. The reporter genes are under the regulatory region that contains a strong constitutive promoter (40SRPS8) and a fucoxanthin-chloroplast protein complex A (FcpA) as terminator.

Saccharomyces cerevisiae VL6–48 (ATCC MYA-3666: MAT*α* his3-Δ200 trp1-Δ1 ura3–52 lys2 ade2–1 met14 cir0) was used for the yeast assembly as described previously [30]. Positive yeast strains containing His selection grew on minimal yeast media without histidine. A pool of the grown yeasts was harvested 5 days after assembly and total DNA was extracted as described previously [32]. Assembled plasmids was then amplified in chemio-competent *Escherichia coli* (Epi300,

Epicenter) grown on Luria Broth (LB) media supplemented with appropriate antibiotic chloramphenicol (25 $mg \cdot L^{-1}$) overnight at 37˚C. Plasmids were then extracted from chloramphenicol-*E. coli* colonies that were tested by colony PCR using a miniprep kit allowing the extraction of large vectors (Biobasic EZ10 miniprep kit, NY, USA). Plasmids were verified by sequencing and then amplified in *E. coli* Epi 300 strain containing pTA-MOB plasmid to allow conjugation with wild type diatoms as described in the literature [30]. Transfer of plasmid DNA to *P. tricornutum* via conjugation from *E. coli* was performed as described [33]. For this, 250 µL of wild type *P. tricornutum* culture were adjusted to a density of 10^8 $cells \cdot mL^{-1}$, this density was obtained by plating 1 mL of wild type *P. tricornutum* on 1/2 × L1 1% agar plates and grown at 18˚C under cool fluorescent lights (75 $\mu mol \cdot m^{-2} \cdot s^{-1}$ on a light/dark cycle of 16/8h) for 4 days. Prior to transformation, 1 mL of L1 media was added to each agar plate, cells were scraped then harvested by pipetting in a sterile tube. Cells were then diluted and mounted in an improved Neubauer hemacytometer (BLAUBRAND® counting chamber, Sigma, USA) to be counted and then cell concentration was adjusted to 5.0×10^8 $cells \cdot mL^{-1}$. A volume of 50 mL *E. coli* culture containing the assembled plasmid and pTA-MOB was grown at 37˚C under agitation to OD_{600nm} of 0.9. Cells were then centrifuged at 3000 g for 10 min and resuspended in 500 µL of SOC media. Conjugation was initiated by adding 200 µL of *P. tricornutum* to 200 µL of *E. coli* cells. The cell mixture was then plated on 1/2 L1, 5% LB, 1% agar plates, incubated at 30˚C for 90 min in the dark and then transferred to 18˚C in the light and grown for 2 days. Two days later, 1 mL of L1 media was added to the plates to collect cells by scrapping and a volume of 200 µL of cells were plated on 1/2 L1, 1% agar plates supplemented with zeocin 50 $\mu g \cdot mL^{-1}$ for selection and incubated at 18˚C under light (75 $\mu mol \cdot m^{-2} \cdot s^{-1}$). Two weeks later, colonies were collected and streaked again on 1/2 L1, 1% agar plates supplemented with zeocin 50 $\mu g \cdot mL^{-1}$. Positive colonies were screened by fluorescence under a Fluorescent Stereo Microscope Leica M165 FC with GFP filter. YFP fluorescence from *P. tricornutum* transconjugants was assessed using the Synergy H1 Bio Tek microplate reader. A volume of 200 µL cell culture transconjugants was measured for fluorescence in black 96 well plate at Ex/Em wavelengths of 500/539nm (n = 3). Strains containing plasmid YFP (17389 bp) and pPtGE30 (16,149 bp) are named here *Pt*YFP and *Pt*ev respectively.

2.3. Flow Cytometry and Fluorescence-Activated Cell Sorting (FACS)

The BD FACS Melody (BD Biosciences, La Jolla, CA, USA) equipped with blue (488 nm), red (640 nm) and violet (405 nm) lasers were used to sort *Pt*YFP cells according to YFP production. Prior to the first sort, selected cells were grown in L1 liquid medium supplemented with Zeocin (50 $\mu g \cdot mL^{-1}$) and grown for 14 days. *P. tricornutum* cultures were washed in L1 medium, filtered on a 100 µm Nylon Net filter (Merck Millipore, Ireland) and diluted to an $OD_{680nm} = 0.1$ in L1 media prior to sorting.

Events were acquired at a fixed flow rate and at least 10,000 events were analysed. Cells were gated according to FSC-A (forward scatter area) and SSC-A (side scatter area) parameters and doublons were excluded according to further gating on homogeneous FSC-H (height) *vs.* FSC-W (width) and SSC-H *vs.* SSC-W populations. Chloroplast autofluorescence was measured on the PerCP channel (700/54nm). Cells with high homogeneous levels of PerCP fluorescence were further gated, whereas cells with high non-specific autofluorescence were excluded based on their emission in 448/45nm channel. YFP was further analysed on the 527/32 nm band-pass filter channel. Sorted cells (1.0×10^5 cells·mL^{-1}) were collected in 1.5 mL tube containing 500 µL of L1 media without antibiotics, centrifuged 10 min at 3500 × g and 90% - 95% of the supernatant was removed and replaced by 500 µL of L1 media supplemented with Zeocin 50 µg·mL^{-1}, chloramphenicol 35 µg·mL^{-1} and ampicillin 100 µg·mL^{-1} to avoid contamination. This was used as inoculum to L1 media 20 mL culture, supplemented with Zeocin 50 µg·mL^{-1}. Ptev cells were used as negative control.

For the second round of sorting, 1st round-sorted cultures were incubated for 11 days and diluted in 1 mL to an OD_{680nm} of 0.1. The cultures were then grown for another 11 days, and sorted, following the same procedure. In this round, non-fluorescent (YFP$^-$) *Pt*YFP cells were sorted too. After the second sorting round, *Pt*YFP YFP$^+$ fluorescent and YFP$^-$ non-fluorescent cells were monitored for 11 and 23 days, respectively to monitor YFP production. Figures and statistics were analyzed using BD FlowJo version 10 software (BD Biosciences, La Jolla, CA, USA, 2020).

2.4. Light Settings

Spectral Quality

We studied the different spectral quality impacts such as (Red 1 (R1), Red 2 (R2) Blue (B), Yellow (Y) and White (C)) on *P. tricornutum* which were provided using the different light or filters. The wavelength absorbed by the filters was obtained by measuring the spectra scanning between 400 - 700 nm using Synergy H1 Microplate Reader, BioTek (**Figure 1**). The transmittance curve is calculated from the absorption curve. $A = 2 - \log_{10}\%T$ (T = Transmittance) therefore, we can calculate the transmittance by undoing the log function (%T = antilog (2 - absorbance)) [34]. We used here different filters (red, blue, yellow), compared to white light as control, to study the impact of different light spectra on growth and lipid. The following conditions were used to study the *P. tricornutum* cell growth trend and lipid accumulation.

Light Intensity

The photon flux density of 65 µmol·m^{-2}·s^{-1} Low light (LL) and 145 µmol·m^{-2}·s^{-1} Medium light (ML) was used in the present study for the effect on growth trend and lipid profile.

Light Shift

The light shift is a strategy where we shift the cultures from one light condition

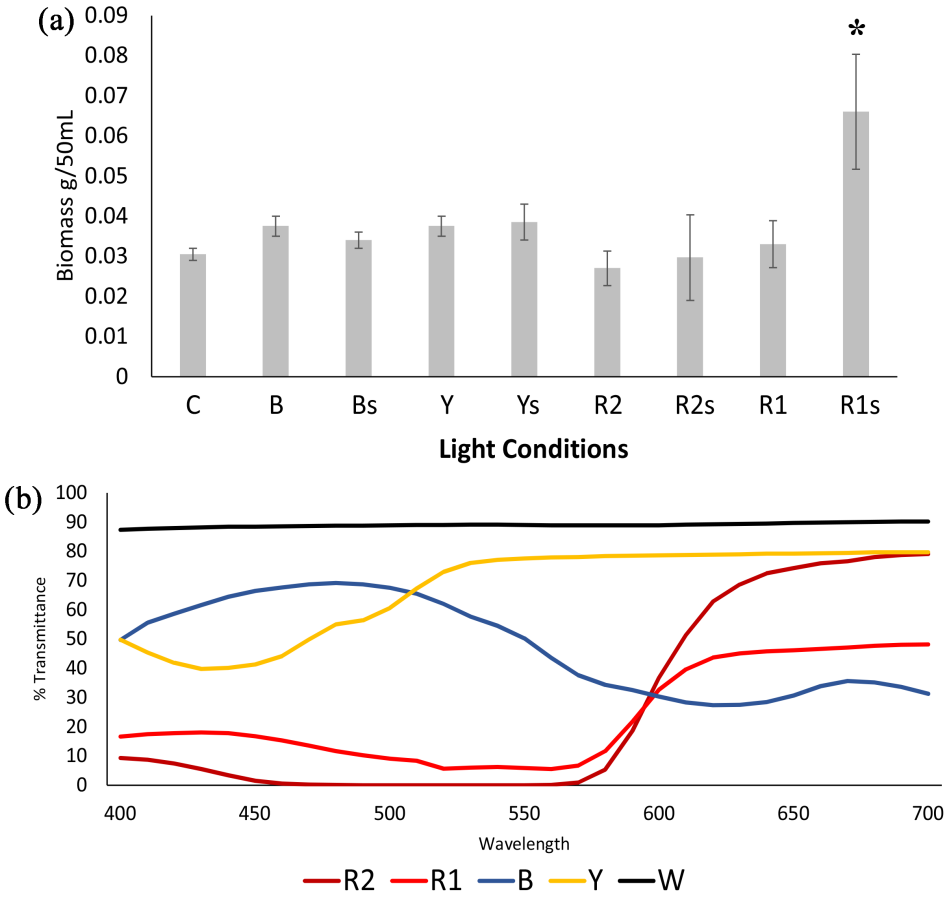

Figure 1. Analysis of *P. tricornutum* biomass (a) and spectral transmittance used (b) under different colors of light. Abbreviations for the conditions are C: white, B: blue, Bs: blue shift, Y: yellow, Ys: yellow shift, R: red R2, Rs: red R2 shift, r: red R1, and rs: red R1 shift. Each bar represents the average of three replicates, and error bars represent standard deviation. *Correspond to significant differences calculated using one-way analysis of variance (ANOVA) followed by a pairwise mean comparison Tukey's test where differences were detected ($n = 3$, $p < 0.05$).

to another condition after a certain period of time. As such, the cultures were grown under red light until they reached an OD_{680mn} of 0.6 absorbance units (*i.e.* 5 - 6 days) and then cultures were shifted from red light to white light to growth until collection. The data of red light shift was compared to data from cultures grown in continuous red light. We performed a pre-screen for all the spectral quality (R1, R2, B, Y and C) and the respective light shift (R1s, R2s, Bs, Ys) to decide on the best light conditions to be used for further optimization (**Figure 1**).

2.5. Lipid Analysis

Total lipid were extracted using Bligh and Dyer method with slight modifications [35]. Briefly, to a 5 mL Eppendorf tube containing a known amount of dry algal biomass, mixtures of methanol and chloroform were added in 2:1 ratio. The mixture was vortexed for 2 min and incubated at room temperature for 24 h, after which 1 mL of chloroform and 0.9 mL of water were added. The mixture was vortexed for 2 min again, and the different layers were separated by centri-

fugation for 10 min at 300 × *g*. The lower layer was evaporated, and the residue was dried at 80˚C for 30 min. The weight was calculated using a precision scale.

Neutral Lipid Detection by Flow Cytometry

Equal volumes of cultures sampled on days 6 and 8 were centrifuged at 10,000 rpm for 10 min. The supernatant was discarded and 10% of DMSO was added. Tubes were vortexed for 30 seconds and centrifuged at 10,000 rpm for 10 min. The supernatant was discarded, and the pellet was mixed with 1 mL of autoclaved milli-Q water. Cultures were further aliquoted to 250 µL in 96 well black plate and 10 µL of Nile red (9-(diethylamino)-5h-benzo[a]phenoxazinone) (0.1 $mg{\cdot}mL^{-1}$ dissolved in acetone) was added. Plates were incubated for 10 min in the dark. The accumulation of intracellular lipid was measured on an FC500 MPL cytometer (Beckman Coulter, Brea, CA, USA) equipped with Air-cooled Argon ion laser, 488 nm and a red solid-state laser, 631 nm. The fluorescence signals of both the control and stained cells were acquired to gate for Nile-Red^{+} cells in the 620 nm/20 FL3 channel. Data was analysed using FlowJo software (FlowJo LLC, Ashland, OR, USA). Other variables like cell size, granulosity and chlorophyll were also measured from different channels.

GC-MS Analysis of Fatty Acids

Fatty acid methyl esters were prepared directly from the wet algal biomass. NaOH in methanol (1 mL of 0.5 N) was added to test tubes containing the biomass; then, the tubes were placed in a sonicating bath for 3 min, followed by heating at 90˚C for 10 min. The samples were allowed to cool, and 1 mL of 1.5% H_2SO_4 in methanol was added. Then, samples were heated again at 90˚C for 10 min. After cooling, 1 mL of water and 1 mL of hexane were added. Test tubes were vortexed for 2 min and then centrifuged at 1200 × *g* for 5 min. The hexane layer containing Fatty acid methyl esters analysis (FAME) was recovered and dried over anhydrous sodium sulphate. FAME was quantified using temperature-programmed gas liquid chromatography on a Scion 436 gas chromatograph fitted with a 30 m × 0.25 mm column coated with 50% cyanopropyl-methylpolysiloxane (DB-23) and linked to a computerized integration system [36]. The fatty acid data were expressed as the mass percent of total fatty acid identified as described previously [22].

2.6. Statistics

All experiments were conducted in triplicate. Statistically significant differences (SD) were identified paired t-test and two-way ANOVA performed on data with a 5% level of probability using Graph Pad Prism software 9.2.0. We have used * to annotate the statistical significance which are as following: *$p \leq 0.05$, **$p \leq 0.01$, ***$p \leq 0.001$.

3. Results

3.1. Effect of Light Characteristics on Cell Growth and Lipid Accumulation of *P. tricornutum* Transconjugant Cells

Diatoms *P. tricornutum* are popular microalgae for the production of biofuels

and lipids. In a previous work, we studied the effect of light on *P. tricornutum* in autotrophic and mixotrophic conditions to promote biomass and lipids accumulation. It was observed that red light and red light shift (*i.e.* substituting white light by red light), impacted biomass yield and lipid content of wild type *P. tricornutum* [22]. With the development of efficient conjugation-based transformation system allowing the introduction of stable episomes [31], *P. tricornutum* has become an ideal platform for metabolic engineering applications such as the production of biofuels and lipids. However, the impact of the presence of an episome and high levels of heterologous proteins on *P. tricornutum* growth or lipid accumulation has not been measured. Similarly, the impact of different light characteristics on *P. tricornutum* transconjugant cells containing an episomal vector has not been investigated.

We first evaluated the effect of different light characteristics (*i.e.* spectral quality, light intensity, and light shift) on *P. tricornutum* transconjugant cells containing an episomal vector (*Ptev*). We confirmed our prior analysis by testing the spectral quality of Red (R), Blue (B), Yellow (Y), White light (C) on biomass (**Figure 1(a)**). Similar to results obtained with *P. tricornutum* wild type cells [22], the only characteristic that significantly impacted the biomass accumulation of *Pt*ev transconjugant cells was red light shift which causing > 1.5 fold increase (**Figure 1(a)**).

To strengthen our knowledge on the effects of the different compositions of red light spectra, we used two types of red (R) filter, *i.e.* R1 with 66 % of transmittance of over 600 nm and in R2 with transmittance spectra of 90 % in over 600 nm (**Figure 1(b)**). When comparing the two R1 and R2 spectra qualities on *Pt*ev biomass and growth, we observed R1 light condition resulted in a more effective biomass accumulation and growth as compared to R2 (**Figure 2(a)**, **Figure 3(a)**). Then, we evaluated the impact of R1 and R2 on the lipid content of *Pt*ev using gravimetric analysis [35]. The average lipid content in R1 was 1.6-fold higher as compared to R2, but the difference was not statistically significant (**Figure 2(b)**). Since R1 significantly increased *Pt*ev biomass and impacted lipid accumulation, R1 was selected for the subsequent experiments.

Next, we investigated the impact of two light intensities, (*i.e.* 65 $\mu mol \cdot m^{-2} \cdot s^{-1}$ and 145 $\mu mol \cdot m^{-2} \cdot s^{-1}$) of R1 filter on *Pt*ev cells by monitoring the growth curve. The results showed that during the lag phase, cell growth did not differ with respect to the initial light intensity, consistently with the fact that this is an adaptation phase. However, the growth rate, as measured at OD_{680nm}, increased at 145 $\mu mol \cdot m^{-2} \cdot s^{-1}$ as compared to 65 $\mu mol \cdot m^{-2} \cdot s^{-1}$ until the end of the exponential phase (**Figure 3(b)**). However, we calculated the dry weight biomass of *Pt*ev and noted that there was no difference between the light intensities (**Figure 2(a)**). Furthermore, we observed that lipid content for spectra R1 at 65 $\mu mol \cdot m^{-2} \cdot s^{-1}$ and 145 $\mu mol \cdot m^{-2} \cdot s^{-1}$, we observed that R1 spectral quality provides a significant increase in lipid accumulation at 145 $\mu mol \cdot m^{-2} \cdot s^{-1}$ as compared to 65 $\mu mol \cdot m^{-2} \cdot s^{-1}$ (**Figure 4**). Thus, we proceeded with R1 at 145 $\mu mol \cdot m^{-2} \cdot s^{-1}$ for our next study.

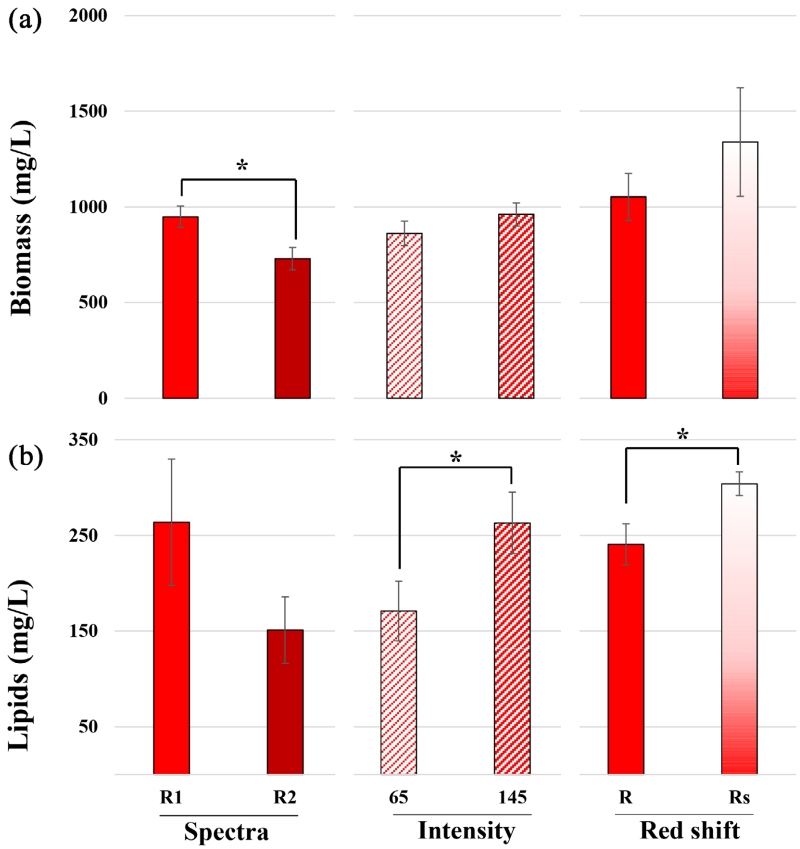

Figure 2. Effect of different light characteristics on *P. tricornutum* cells growth and lipid accumulation. The effect on (a) biomass—dry weight (mg/L) and on (b) lipids accumulation as measured by the Bligh and Dyer method was determined. The different light characteristics includes spectra: shows the effect of the exposure to spectra quality R1 (34% > 600 nm > 66%) and R2 (8% > 600 nm > 92%), intensity: shows the effect of the exposure to light intensities of 65 and 145 $\mu mol \cdot m^{-2} \cdot s^{-1}$ and shift: with the light conditions of continuous red light (RL) and red light shift (RLS). All data points are presented as a mean of triplicates with standard deviation (n = 3). *Statistically different using two-way Anova, $p < 0.05$.

We further investigated two shortlisted conditions red light spectra (R) and red light shift (Rs) (from red to white light spectra) on *Pt*ev cells based on previous results obtained with *P. tricornutum* wild type cells [22]. Results showed that *Pt*ev biomass accumulates in both, R and Rs conditions, however the accumulation of lipids was significantly higher in Rs (**Figure 2(b)**).

3.2. Effect of Red and Red Light Shift on Cell Growth and Lipid Accumulation in Different *P. tricornutum* Transconjugants

P. tricornutum transconjugant cells represent an interesting biotechnological alternative for the production of various biomolecules such as lipids however, the impact of the episome and the expression of its inserted genes on *P. tricornutum* transconjugant is not known. As such, we investigated the effect of the above selected Rs condition on *Pt*ev and on *P. tricornutum* transconjugant cells containing the same episomal vector but to which the yellow fluorescent protein (YFP)

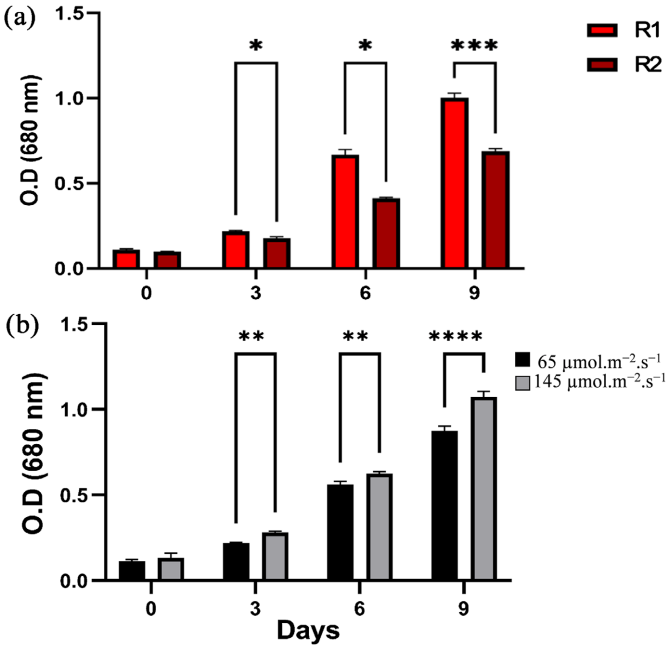

Figure 3. Analysis of the growth of *P. tricornutum* transconjugant cells containing an empty episomal vector (*Pt*ev) following (a) the effect of two different spectra quality where R1 (34% > 600 nm > 66%) and R2 (8% > 600 nm > 92%) and (b) the exposure to two different light intensities of 65 and 145 µmol·m^{-2}·s^{-1}. Each bar represents the average of three replicates, and error bars represent standard deviation. Statistically significant differences were identified using a paired t-test and two-way ANOVA performed on data with a 5% level of probability. We have used * to annotate the statistical significance which are as following: *p ≤ 0.05, **p ≤ 0.01, ***p ≤ 0.001, ****p ≤ 0.00001.

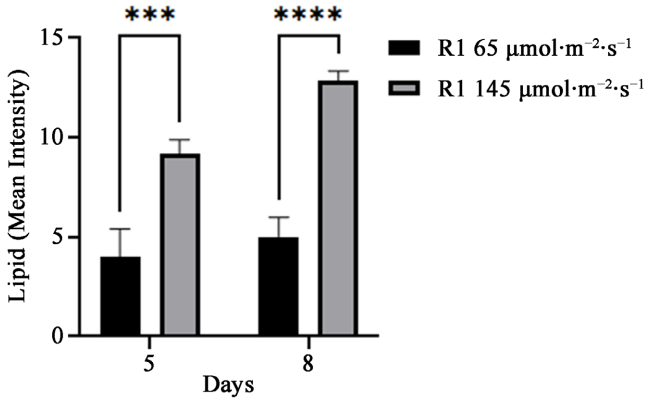

Figure 4. Analysis of lipid content for *Pt*ev under two red light intensity 65 µmol·m^{-2}·s^{-1} and 145 µmol·m^{-2}·s^{-1} on day 5 and day 8. We have used * to annotate the statistical significance which are as following: *p ≤ 0.05, **p ≤ 0.01, ***p ≤ 0.001, ****p ≤ 0.00001.

reporter gene under the control of a strong constitutive promoter was added. Thus, in addition to have to replicate an episome like *Pt*ev cells, *Pt*YFP cells express and accumulate recombinant proteins. In order to select cells with high levels of heterologous recombinant protein YFP, the *Pt*YFP transconjugant cells used in this study were obtained after repetitive sorting rounds of FACS that ensured the enrichment of the YFP fluorescence as described in materials and

method section. *Pt*YFP cells used in this study were from the 2nd sorting round of selection and displayed 76.88% of fluorescent cells (Figure 5, middle panels).

In the above-mentioned results, we further investigated the effect of the two shortlisted conditions R and Rs on the growth of *Pt*ev and *Pt*YFP transconjugant

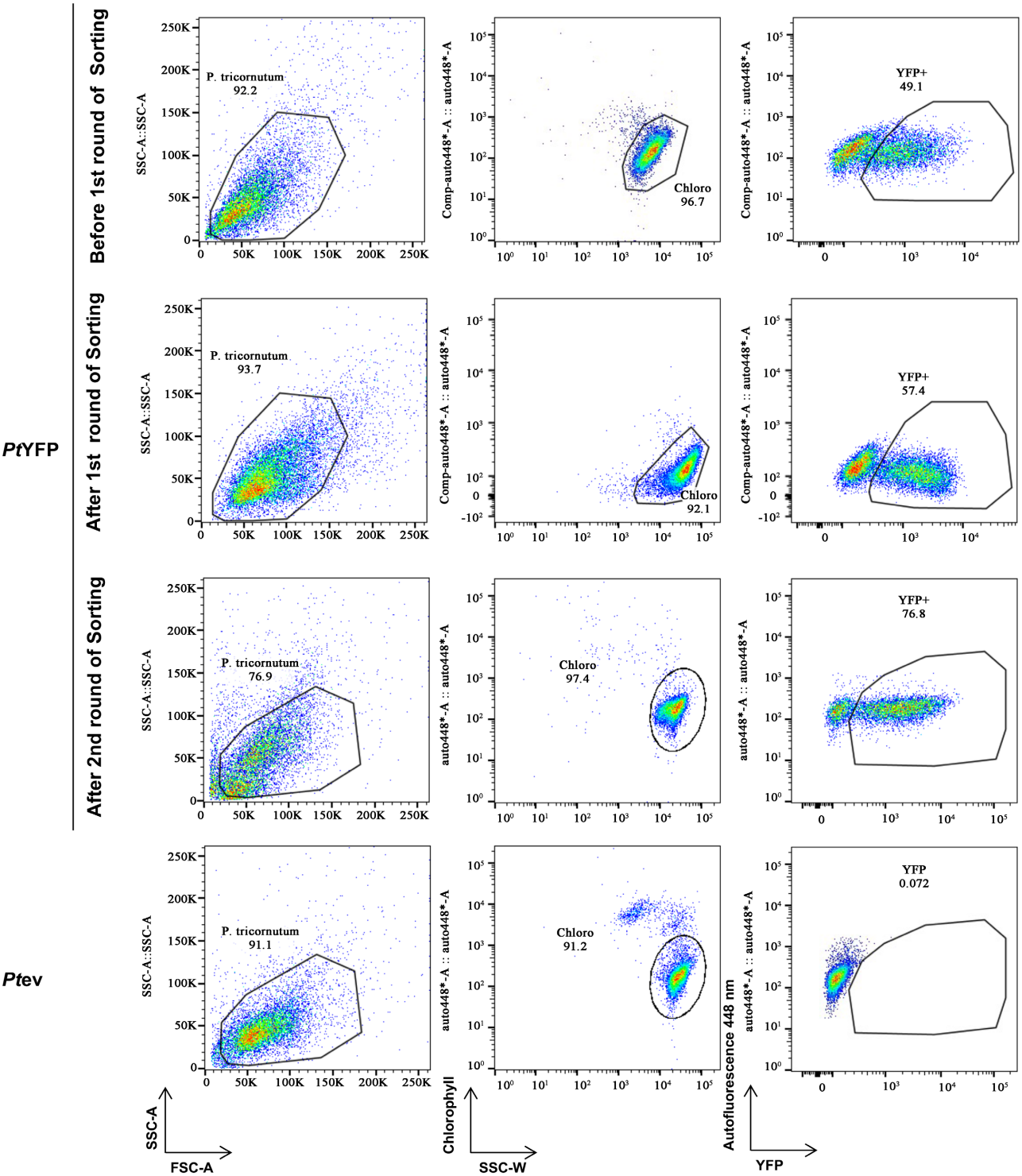

Figure 5. FACS analysis of *P. tricornutum* transconjugant cells containing an empty episomal vector (*Pt*ev) and an episomal vector expressing the reporter gene YFP (*Pt*YFP) and cell sorting.

cells. It was observed that the growth trend in transconjugant containing the reporter gene (*Pf*YFP) was slow as compared to without reporter gene (*Pt*ev). The growth for *Pf*YFPR was significantly slower as compared to *Pt*evR and *Pt*evRs for days 3, 4, 5, 6, 7, 8, 9, 11 (Figure 6(a)). After day 5, culture were shifted to white light (Rs,) and it was observed that after the light shift, PtevRs growth was

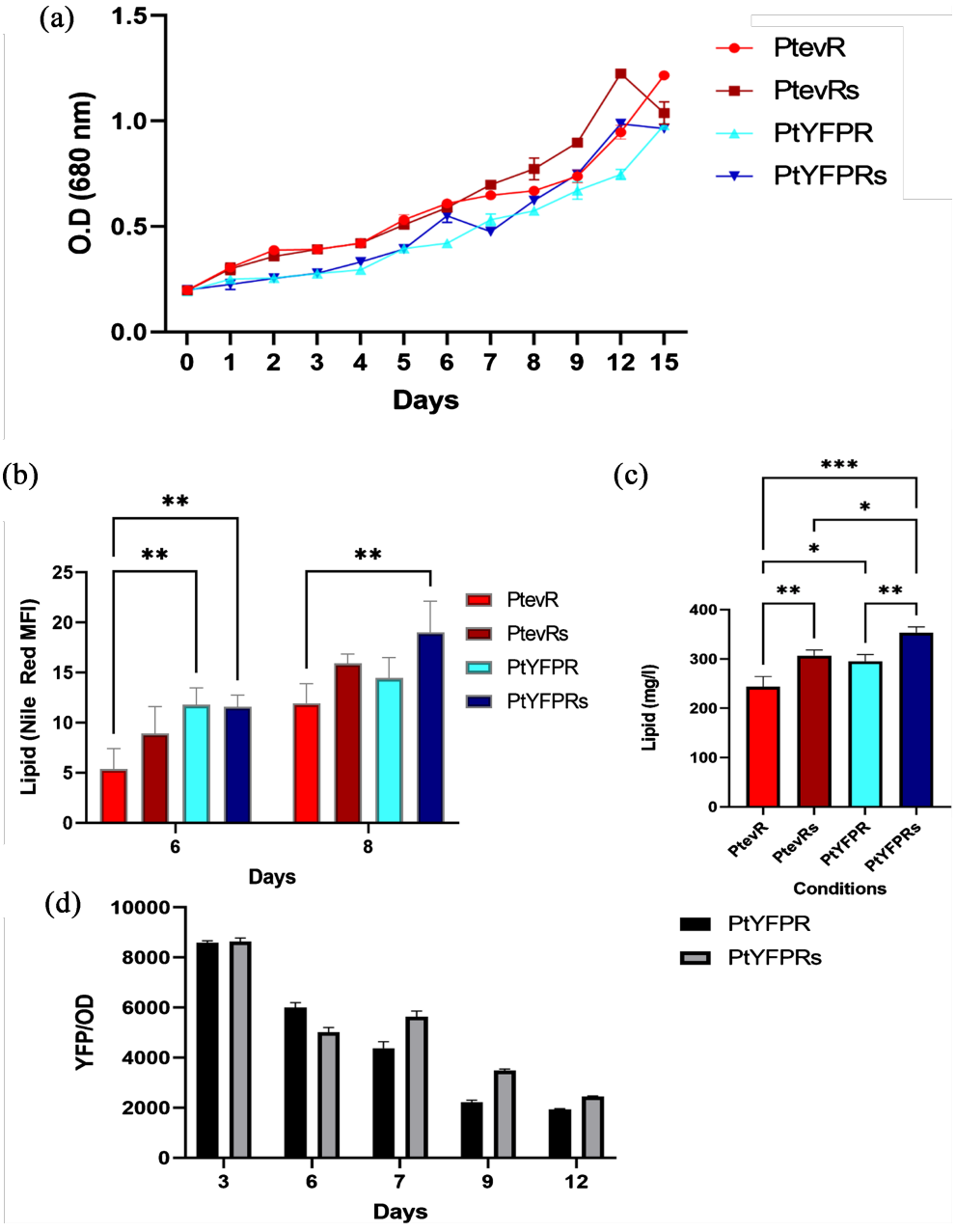

Figure 6. Effect of two different light conditions Red light (R) and Red light shift (Rs) on *P. tricornutum* transconjugant cells containing an empty episomal vector (*Pt*ev) and an episomal vector harboring the Yellow Fluorescent Protein reporter gene (*Pf*YFP). (a) Growth curve over 15 days of *P. tricornutum* transconjugant cells *Pt*ev and *Pf*YFP. (b) Lipid estimation by Nile Red staining and measured by flow cytometer (Mean Fluorescence intensity; MFI). (c) Dry weight lipid estimation using gravimetric method on day 8. (d) Ratio of the fluorescence YFP over the number of cells for *Pf*YFP growth in R and Rs conditions.

significantly higher as compared to *Pt*YFPR on day 6, 7, 8, and 11.

Lipid accumulation at day 6 and 8 was then measured by Nile red staining analysis using a flow cytometer and dry weight estimation using Bligh and Dyer method (Figure 6(b), Figure 6(c)). As previously noted, lipid accumulated in higher amounts when *Pt*ev was submitted to Rs (Figure 2(b); Figure 6(b), Figure 6(c)). Interestingly, there was more lipids per cell in *Pt*YFP as compared to *Pt*ev for all conditions at both day 6 and 8, although results were only significant when comparing *Pt*evR with *Pt*YFP-R and *Pt*YFP-Rs (Figure 6(b)). Even though, the data was bit different when compared with dry weight lipid on day 8, the data showed that Rs was effective and significantly increased the total lipid in both *Pt*ev and *Pt*YFP (Figure 6(c)).

We also observed the impact of R and Rs on total YFP fluorescence of *Pt*YFP-R and *Pt*YFP-Rs. Results showed a max fluorescence intensity at day 3 for the two recombinant strains (Figure 6(d)). The difference in fluorescence coming out of the transconjugants cultures could be related to difference in protein accumulation or rearranged episomes which has been discussed in discussion.

Interestingly, we observed more granulosity in R1 as compared to R2 (Figure 7).

3.3. Fatty Acid Composition of *Pt*ev and *Pt*YFP in Red and Red Light Shift

The fatty acid (FA) composition of *Pt*ev and *Pt*YFP cells grown under R and Rs condition showed no significant differences (Table 1 and Table 2). The FA composition (% of total FA) for *Pt*ev and *Pt*YFP in R and Rs condition are similar and showed a highest abundance (44.66% - 50.30%) of polyunsaturated fatty acids (PUFA) (Table 1), whereas monounsaturated fatty acids (MUFA) and saturated fatty acids (SFA) are in same abundance level (around 25% each). These results are comparable to those previously described for *P. tricornutum* wild type [22].

The exact fatty acids identified from *Pt*ev and *Pt*YFP are summarized in Table 2.

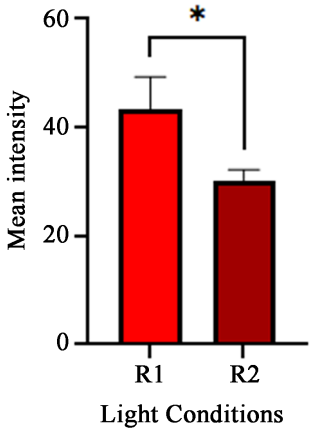

Figure 7. Mean intensity of cell granulosity calculated using FACS for *Pt*ev in R1 and R2. *$p \leq 0.05$.

Table 1. Fatty acid (FA) composition (mass % of total FA identified) analysed by gas chromatography (GC) with Flame-Ionization Detection (GC-FID) from *Pt*ev and *Pf*YFP biomass under two light conditions (R and Rs) on Day 9 (n = 3).

Fatty acids	*Pt*evR	*Pt*evRs	*Pf*YFPR	*Pf*YFPRs
SFA	24.2 ± 3.23	24 ± 1.04	27.55 ± 4.2	27.05 ± 4.25
MUFA	27.69 ± 1.33	25.7 ± 1.13	27.79 ± 2.93	27.84 ± 3.03
PUFA	48.11 ± 7.63	50.30 ± 2.21	44.66 ± 8.63	45.11 ± 9.29
Total	100.00	100.00	100.00	100.00

Table 2. Major fatty acid composition of total lipid in *Pt*ev and *Pf*YFP Red light (R) and Red light shift (Rs). Data are the mean ± standard deviation (SD) of three replicates (n = 3).

Fatty acid name	Fatty acid formula	*Pt*evR	*Pt*evRs	*Pf*YFPR	*Pf*YFPRs
Myristic acid	14:0	7.16 ± 0.03	7.38 ± 0.17	7.53 ± 0.20	7.45 ± 0.33
Palmitic acid	16:0	15.73 ± 2.74	15.24 ± 0.69	18.03 ± 3.32	17.73 ± 3.24
Palmitoleic acid	16:1n-7	23.63 ± 0.32	21.01 ± 0.35	22.97 ± 0.47	21.57 ± 0.84
Stearic acid	18:0	0.58 ± 0.3	0.55 ± 0.12	1.17 ± 0.50	1.07 ± 0.55
Oleic acid	18:1n-9	0.42 ± 0.14	0.58 ± 0.35	0.89 ± 0.37	1.36 ± 0.86
Eicosapentaenoic acid	20:5n-3	20.99 ± 4.31	24.23 ± 0.58	18.5 ± 3.6	20.04 ± 4.52
Docosahexaenoic acid	22:6n-3	1.98 ± 0.17	2.36 ± 0.06	1.40 ± 0.20	1.75 ± 0.35

The main FA components for all samples analyzed in this study were mid- and long-chain FAs, 14:0, 16:0, 16:1n-7, and 20:5n-3. Palmitoleic acid (16:1n-7) was predominant, compared to the other FAs, in all samples under R and Rs light conditions tested. The only FA that was significantly different was eicosapentaenoic acid (EPA), with *Pt*evRs displaying the maximum amount of EPA as compared to other cultures (Two-way ANOVA, $P < 0.05$).

4. Discussion

Diatoms are affected by different conditions and light is one of the important factors. Growth and biomass tend to increase with precise light and culture conditions whereas lipid tends to increase under stress conditions. Moreover, the photosynthetic apparatus in diatoms are distinctly different as compared to green algae and plants, which provides us with an alternative route to produce biomass for industrial use. Recent advances in both physiochemical and synthetic biology, prompted many researchers to investigate *P. tricornutum* for their potential to produce lipids and fatty acids. This study reports on the impact of light characteristics on transconjugants *Pt*ev and *Pf*YFP on growth, lipid and fatty acid composition. Our analysis on transconjugants showed that light characteristics can have subtle impact on growth, lipid and fatty acid profiles.

We showed that there was a significant increase in both growth and harvested biomass for *Ptev* in R1 as compared to R2 (Figure 1, Figure 2). Previously, Valle

et al. and Yi *et al.* and co-authors showed that optimal red: blue ratio can improve light harvesting efficiency [19] [23].

We also observed cell granuolosity, which is affected by the cell morphology and chemical composition such as starch and lipid [37] and we noticed a significant increase in granulosity in R1 as compared to R2 which characterizes the optical complexity of the cell which is dependent on particulate matter inside the cell (**Figure 7**) [38]. There are few plausible explanations to this including a possible change in the thylakoid structure in different light conditions [39] or a change in the curvature of endoplasmic reticulum during lipid droplet expansion [40]. Although the exact mechanism is unclear, the importance of the quantity of red light spectra on growth and fucoxanthin accumulation [41] and lipid synthesis [42] [43] has been well reported and is in support with our results.

Considering the light intensity, it was observed that tested light conditions LL and ML have shown no difference in the total biomass but a significant increase in total lipid in ML (**Figures 2-4**). Even though high growth rate was observed for ML during the exponential phase, it was expected to yield higher biomass, which was not observed (**Figure 2(a)**). Although, there are few studies reported on faster growth trend of *P. tricornutum* in medium light intensity, as compared to low and high light intensity [23] [44] [45]. It has been shown the non-photochemical energy intensity is higher in ML (300 $\mu mol \cdot m^{-2} \cdot s^{-1}$) as compared to LL (30 $\mu mol \cdot m^{-2} \cdot s^{-1}$) which might be one of the reasons for the decrease in total biomass in our experiment [44]. Therefore, part of incoming light energy may be getting dissipated as heat energy when cultures are grown in 145 $\mu mol \cdot m^{-2} \cdot s^{-1}$. Alternatively, it can also be said that light use efficiency is more effective under LL (65 $\mu mol \cdot m^{-2} \cdot s^{-1}$) which has been mentioned by Li *et al.* [45]. This suggests that light intensity between 120 and 220 $\mu mol \cdot m^{-2} \cdot s^{-1}$ is an optimal choice for *P. tricornutum* however for various industrial applications, it is subject to further optimization based on bioreactor-based observations.

We observed that the R1 spectral quality at 65 $\mu mol \cdot m^{-2} \cdot s^{-1}$ and 145 $\mu mol \cdot m^{-2} \cdot s^{-1}$ affected the total lipid accumulation (**Figure 4**). Other studies have reported on the effect of light characteristics on diatoms. For example, it was reported that fucoxanthin, chlorophyll *a* and beta-cryptoxanthin content decreased at 255 $\mu mol \cdot m^{-2} \cdot s^{-1}$ red light as compared to 128 $\mu mol \cdot m^{-2} \cdot s^{-1}$ red light [23]. Also, light shifts increased the biomass, lipid and fucoxanthin content in diatoms [10] [22] [41]. Thus, light intensity of a specific light quality can change the compositions of metabolites such as pigments and lipids.

Here, the light characteristics promoting lipid accumulation [spectral quality—R1 and light intensity-145 $\mu mol \cdot m^{-2} \cdot s^{-1}$ with red light shift], were selected to study the effect on *P. tricornutum* transconjugants (*Pt*ev and *Pt*YFP), the latter accumulating reporter fluorescent proteins. Fluorescent proteins are known to have a noticeable impact on various cellular events [27] [46] [47]. Studies reported on the use of GFP and YFP to enhance the overall spectral coverage and increase the light-harvesting efficiency in *P. tricornutum* and *Rhodobacter sphaeroides*. It was reported that only 5% of the total photons are converted to bio-

mass in diatoms, thus cells may manipulate the spectral composition to reduce the wastage of excess light by using fluorescent proteins [27] [28]. Here, we assessed if the episomal vector along with the reporter gene YFP could have an impact on growth, biomass, lipid and fatty acid profiles.

The growth of the *Pf*YFP transconjugants was significantly slower as compared to *Pt*ev in both R and Rs (**Figure 6**). This could be discussed in two different contexts *i.e.*, replication of episomal vector and fluoroscence of YFP. The size of episomal vector and fluorescence of YFP could negatively affect *P. tricornutum* by extra energy consumption or dissipation and therefore leading to a slow cell division rate (**Figure 6**). It has been reported that rate of replication in episomal vector is comparable to native nuclear *P.tricornutum* and have reported the stability of episomes for 4 weeks but no enzymatic activity for the heterologous protein [30]. A study has reported the comparable growth between transgenic controls, wild type and episome containing heterologous gene with a reporter gene mVenus which is a fluorescent protein [48]. The same study observed the impact of continuous light or light/dark on culture and found no change in the mVenus fluorescence.

Also, it is known that YFP emits yellow fluorescence which is not the suitable wavelength to be absorbed by accessory pigment fucoxanthin and reduces the overall photosynthesis efficiency [49]. The fluorescent proteins are not just sensitive to light conditions but conditions such as pH, chloride ion concentration, pressure and temperature, which can affect the expression of fluorescent proteins [50] [51] [52]. Therefore, there is a small possibility that the change in light conditions might affect the overall accumulation of proteins or total fluorescence inside the cells by modulating the intracellular spectral composition (**Figure 6(d)**).

Diatoms induce the biosynthesis of lipid droplets under various stress and culture conditions such as light [53] [54] and nitrogen limitation [55]. Here, we showed that *Pf*YFP has slower growth in both Red light and Red light shift as compared to *Pt*ev but have shown a significant increase in lipid accumulation on day 6 and 8 in both light conditions (**Figure 6**).

For wild type *P. tricornutum*, it was observed that total biomass and lipid was increased by 2 and 2.3 fold respectively in Red light shift which is indeed more as compared to both transconjugants studied in this investigation [22]. Furthermore, there was a decrease in total polyunsaturated fatty acids in YFP transconjugants along with a significant decrease in EPA, which is one of the major polyunsaturated fatty acids in *P. tricornutum* (**Table 1**). Generally, the increase in unsaturated fatty acids or specifically EPA is known to have an important function in the structure of the thylakoid membrane and regulating photosynthesis such as high pool of EPA in glycerolipids like sulfoquinovosyl diacylglycerides associated with crucial activities like photosynthesis, energy transduction and plastid membranes [56] [57] [58]. Red light spectra was shown to increase specific fatty acids such as hexadecatrienoic acid (16:3) and eicosapentaenoic acid (EPA) (20:5), which might be due to induction phospholipase activity [59].

This study reported on the effect of light characteristics on transconjugants growth, lipids and fatty acid composition. The data obtained from this study shows small differences between *P. tricornutum*, transconjugants carrying, or not, a reporter fluorescent protein.

Acknowledgements

We acknowledge that financial support for this research was funded by the Natural Sciences and Engineering Research Council of Canada through the Alliance program Award No ALLRP 554429-20 and ALLRP 570476-2021 to I.D-P. Additional support in the form of scholarships to N.S., E.F., F.A. and A.A. from Mitacs—Acceleration program grants no IT12310, IT16463 and IT19432 to I.D-P. is also acknowledged.

Authors Contributions

N.S., F.M. and I.D-P. contributed to the study conception and design. Methodology, material preparation, data collection and analysis were performed by N.S., E.F., F.A., N.M., A.A. and F.M. The first draft of the manuscript was written by N.S. E.F., F.A., N.M., A.A. and F.M. edited previous versions of the manuscript. I.D-P. supervised the project and secure funding. All authors read and approved the final manuscript.

Conflicts of Interest

The authors declare no conflicts of interest regarding the publication of this paper.

References

[1] Muscat, A., de Olde, E.M., Ripoll-Bosch, R., Van Zanten, H.H.E., Metze, T.A.P., Termeer, C.J.A.M., van Ittersum, M.K. and de Boer, I.J.M. (2021) Principles, Drivers and Opportunities of a Circular Bioeconomy. *Nature Food*, **2**, 561-566. https://doi.org/10.1038/s43016-021-00340-7

[2] Li, H.-Y., Lu, Y., Zheng, J.-W., Yang, W.-D. and Liu, J.-S. (2014) Biochemical and Genetic Engineering of Diatoms for Polyunsaturated Fatty Acid Biosynthesis. *Marine Drugs*, **12**, 153-166. https://doi.org/10.3390/md12010153

[3] Monika Prakash, R., Trishnamoni, G. and Nikunj, S. (2015) Effect of Salinity, pH, Light Intensity on Growth and Lipid Production of Microalgae for Bioenergy Application. *OnLine Journal of Biological Sciences*, **15**, 260-267. https://doi.org/10.3844/ojbsci.2015.260.267

[4] Benedetti, M., Vecchi, V., Barera, S. and Dall'Osto, L. (2018) Biomass from Microalgae: The Potential of Domestication towards Sustainable Biofactories. *Microbial Cell Factories*, **17**, 173. https://doi.org/10.1186/s12934-018-1019-3

[5] Sharma, N., Simon, D.P., Diaz-Garza, A.M., Fantino, E., Messaabi, A., Meddeb-Mouelhi, F., Germain, H. and Desgagné-Penix, I. (2021) Diatoms Biotechnology: Various Industrial Applications for a Greener Tomorrow. *Frontiers in Marine Science*, **8**, Article ID: 636613. https://doi.org/10.3389/fmars.2021.636613

[6] Dhaouadi, F., Awwad, F., Diamond, A. and Desgagne-Penix, I. (2020) Diatoms' Break-

throughs in Biotechnology: *Phaeodactylum tricornutum* as a Model for Producing High-Added Value Molecules. *American Journal of Plant Sciences*, **11**, 1632-1670. https://doi.org/10.4236/ajps.2020.1110118

[7] Yu, A.-Q., Pratomo Juwono, N.K., Leong, S.S.J. and Chang, M.W. (2014) Production of Fatty Acid-Derived Valuable Chemicals in Synthetic Microbes. *Frontiers in Bioengineering and Biotechnology*, **2**, 78. https://doi.org/10.3389/fbioe.2014.00078

[8] Jin, and Agustí, S. (2018) Fast Adaptation of Tropical Diatoms to Increased Warming with Trade-Offs. *Scientific Reports*, **8**, Article No. 17771. https://doi.org/10.1038/s41598-018-36091-y

[9] Koehne, B., Elli, G., Jennings, R.C., Wilhelm, C. and Trissl, H.W. (1999) Spectroscopic and Molecular Characterization of a Long Wavelength Absorbing Antenna of Ostreobium sp. *Biochimica et Biophysica Acta* (*BBA*)—*Bioenergetics*, **1412**, 94-107. https://doi.org/10.1016/S0005-2728(99)00061-4

[10] Jungandreas, A., Schellenberger Costa, B., Jakob, T., von Bergen, M., Baumann, S. and Wilhelm, C. (2014) The Acclimation of *Phaeodactylum tricornutum* to Blue and Red Light Does Not Influence the Photosynthetic Light Reaction but Strongly Disturbs the Carbon Allocation Pattern. *PLOS ONE*, **9**, e99727. https://doi.org/10.1371/journal.pone.0099727

[11] Lehmuskero, A., Skogen Chauton, M. and Boström, T. (2018) Light and Photosynthetic Microalgae: A Review of Cellular- and Molecular-Scale Optical Processes. *Progress in Oceanography*, **168**, 43-56. https://doi.org/10.1016/j.pocean.2018.09.002

[12] Taddei, L., Chukhutsina, V.U., Lepetit, B., Stella, G.R., Bassi, R., van Amerongen, H., Bouly, J.-P., Jaubert, M., Finazzi, G. and Falciatore, A. (2018) Dynamic Changes between Two LHCX-Related Energy Quenching Sites Control Diatom Photoacclimation. *Plant Physiology*, **177**, 953-965. https://doi.org/10.1104/pp.18.00448

[13] Oka, K., Ueno, Y., Yokono, M., Shen, J.-R., Nagao, R. and Akimoto, S. (2020) Adaptation of Light-Harvesting and Energy-Transfer Processes of a Diatom *Phaeodactylum tricornutum* to Different Light Qualities. *Photosynthesis Research*, **146**, 227-234. https://doi.org/10.1007/s11120-020-00714-1

[14] Lockhart, J. (2013) Blue Light Checkpoint: How Blue Light Controls the Onset of Cell Division in Diatoms. *The Plant Cell*, **25**, 1. https://doi.org/10.1105/tpc.113.250110

[15] Schellenberger Costa, B., Jungandreas, A., Jakob, T., Weisheit, W., Mittag, M. and Wilhelm, C. (2012) Blue Light Is Essential for High Light Acclimation and Photoprotection in the Diatom *Phaeodactylum tricornutum*. *Journal of Experimental Botany*, **64**, 483-493. https://doi.org/10.1093/jxb/ers340

[16] Büchel, C., Wilhelm, C., Wagner, V. and Mittag, M. (2017) Functional Proteomics of Light-Harvesting Complex Proteins under Varying Light-Conditions in Diatoms. *Journal of Plant Physiology*, **217**, 38-43. https://doi.org/10.1016/j.jplph.2017.06.007

[17] De Tommasi, E. (2016) Light Manipulation by Single Cells: The Case of Diatoms. *Journal of Spectroscopy*, **2016**, Article ID: 2490128. https://doi.org/10.1155/2016/2490128

[18] Carvalho, A.P., Silva, S.O., Baptista, J.M. and Malcata, F.X. (2011) Light Requirements in Microalgal Photobioreactors: An Overview of Biophotonic Aspects. *Applied Microbiology and Biotechnology*, **89**, 1275-1288. https://doi.org/10.1007/s00253-010-3047-8

[19] Valle, K.C., Nymark, M., Aamot, I., Hancke, K., Winge, P., Andresen, K., Johnsen, G., Brembu, T. and Bones, A.M. (2014) System Responses to Equal Doses of Photosynthetically Usable Radiation of Blue, Green, and Red Light in the Marine Diatom

Phaeodactylum tricornutum. *PLOS ONE*, **9**, e114211. https://doi.org/10.1371/journal.pone.0114211

[20] Véron, B., Billard, C., Dauguet, J.-C. and Hartmann, M.-A. (1996) Sterol Composition of *Phaeodactylum tricornutum* as Influenced by Growth Temperature and Light Spectral Quality. *Lipids*, **31**, 989-994. https://doi.org/10.1007/BF02522694

[21] Villanova, V., Singh, D., Pagliardini, J., Fell, D., Le Monnier, A., Finazzi, G. and Poolman, M. (2021) Boosting Biomass Quantity and Quality by Improved Mixotrophic Culture of the Diatom *Phaeodactylum tricornutum*. *Frontiers in Plant Science*, **12**, Article ID: 642199. https://doi.org/10.3389/fpls.2021.642199

[22] Sharma, N., Fleurent, G., Awwad, F., Cheng, M., Meddeb-Mouelhi, F., Budge, S.M., Germain, H. and Desgagné-Penix, I. (2020) Red Light Variation an Effective Alternative to Regulate Biomass and Lipid Profiles in *Phaeodactylum tricornutum*. *Applied Sciences*, **10**, 2531. https://doi.org/10.3390/app10072531

[23] Yi, Z., Su, Y., Cherek, P., Nelson, D.R., Lin, J., Rolfsson, O., Wu, H., Salehi-Ashtiani, K., Brynjolfsson, S. and Fu, W. (2019) Combined Artificial High-Silicate Medium and LED Illumination Promote Carotenoid Accumulation in the Marine Diatom *Phaeodactylum tricornutum*. *Microbial Cell Factories*, **18**, 209. https://doi.org/10.1186/s12934-019-1263-1

[24] Conceição, D., Lopes, R.G., Derner, R.B., Cella, H., do Carmo, A.P.B., Montes D'Oca, M.G., Petersen, R., Passos, M.F., Vargas, J.V.C., Galli-Terasawa, L.V. and Kava, V. (2020) The Effect of Light Intensity on the Production and Accumulation of Pigments and Fatty Acids in *Phaeodactylum tricornutum*. *Journal of Applied Phycology*, **32**, 1017-1025. https://doi.org/10.1007/s10811-019-02001-6

[25] D'Adamo, S., Schiano di Visconte, G., Lowe, G., Szaub-Newton, J., Beacham, T., Landels, A., Allen, M.J., Spicer, A. and Matthijs, M. (2019) Engineering the Unicellular Alga *Phaeodactylum tricornutum* for High-Value Plant Triterpenoid Production. *Plant Biotechnology Journal*, **17**, 75-87. https://doi.org/10.1111/pbi.12948

[26] Hamilton, M.L., Haslam, R.P., Napier, J.A. and Sayanova, O. (2014) Metabolic Engineering of *Phaeodactylum tricornutum* for the Enhanced Accumulation of Omega-3 Long Chain Polyunsaturated Fatty Acids. *Metabolic Engineering*, **22**, 3-9. https://doi.org/10.1016/j.ymben.2013.12.003

[27] Fu, W., Chaiboonchoe, A., Khraiwesh, B., Sultana, M., Jaiswal, A., Jijakli, K., Nelson, D.R., Al-Hrout, A.a., Baig, B., Amin, A. and Salehi-Ashtiani, K. (2017) Intracellular Spectral Recompositioning of Light Enhances Algal Photosynthetic Efficiency. *Science Advances*, **3**, e1603096. https://doi.org/10.1126/sciadv.1603096

[28] Grayson, K.J., Faries, K.M., Huang, X., Qian, P., Dilbeck, P., Martin, E.C., Hitchcock, A., Vasilev, C., Yuen, J.M., Niedzwiedzki, D.M., Leggett, G.J., Holten, D., Kirmaier, C. and Neil Hunter, C. (2017) Augmenting Light Coverage for Photosynthesis through YFP-Enhanced Charge Separation at the *Rhodobacter sphaeroides* Reaction Centre. *Nature Communications*, **8**, 13972. https://doi.org/10.1038/ncomms13972

[29] Seo, S., Kim, J., Lee, J.-W., Nam, O., Chang, K.S. and Jin, E. (2020) Enhanced Pyruvate Metabolism in Plastids by Overexpression of Putative Plastidial Pyruvate Transporter in *Phaeodactylum tricornutum*. *Biotechnology for Biofuels*, **13**, 120. https://doi.org/10.1186/s13068-020-01760-6

[30] Karas, B.J., Diner, R.E., Lefebvre, S.C., McQuaid, J., Phillips, A.P.R., Noddings, C.M., Brunson, J.K., Valas, R.E., Deerinck, T.J., Jablanovic, J., Gillard, J.T.F., Beeri, K., Ellisman, M.H., Glass, J.I., Hutchison Iii, C.A., Smith, H.O., Venter, J.C., Allen, A.E., Dupont, C.L. and Weyman, P.D. (2015) Designer Diatom Episomes Delivered by Bacterial Conjugation. *Nature Communications*, **6**, 6925.

https://doi.org/10.1038/ncomms7925

[31] Slattery, S.S., Diamond, A., Wang, H., Therrien, J.A., Lant, J.T., Jazey, T., Lee, K., Klassen, Z., Desgagné-Penix, I., Karas, B.J. and Edgell, D.R. (2018) An Expanded Plasmid-Based Genetic Toolbox Enables Cas9 Genome Editing and Stable Maintenance of Synthetic Pathways in *Phaeodactylum tricornutum*. *ACS Synthetic Biology*, **7**, 328-338. https://doi.org/10.1021/acssynbio.7b00191

[32] Kouprina, N., Lee, N.C.O., Kononenko, A.V., Samoshkin, A. and Larionov, V. (2015) From Selective Full-Length Genes Isolation by TAR Cloning in Yeast to Their Expression from HAC Vectors in Human Cells. In: Narayanan, K., Ed., *Bacterial Artificial Chromosomes*, Springer, New York, 3-26. https://doi.org/10.1007/978-1-4939-1652-8_1

[33] Karas, B.J., Jablanovic, J., Sun, L., Ma, L., Goldgof, G.M., Stam, J., Ramon, A., Manary, M.J., Winzeler, E.A., Venter, J C., Weyman, P.D., Gibson, D.G., Glass, J.I., Hutchison, C.A., Smith, H.O. and Suzuki, Y. (2013) Direct Transfer of Whole Genomes from Bacteria to Yeast. *Nature Methods*, **10**, 410-412. https://doi.org/10.1038/nmeth.2433

[34] Gilbert, P.U.P.A. and Haeberli, W. (2007) Experiments on Subtractive Color Mixing with a Spectrophotometer. *American Journal of Physics*, **75**, 313-319. https://doi.org/10.1119/1.2431654

[35] Bligh, E.G. and Dyer, W.J. (1959) A Rapid Method of Total Lipid Extraction and Purification. *Canadian Journal of Biochemistry and Physiology*, **37**, 911-917. https://doi.org/10.1139/y59-099

[36] Budge, S.M., Iverson, S.J. and Koopman, H.N. (2006) Studying Trophic Ecology in Marine Ecosystems Using Fatty Acids: A Primer on Analysis and Interpretation. *Marine Mammal Science*, **22**, 759-801. https://doi.org/10.1111/j.1748-7692.2006.00079.x

[37] Hyka, P., Lickova, S., Přibyl, P., Melzoch, K. and Kovar, K. (2013) Flow Cytometry for the Development of Biotechnological Processes with Microalgae. *Biotechnology Advances*, **31**, 2-16. https://doi.org/10.1016/j.biotechadv.2012.04.007

[38] Fernández-Castané, A., Li, H., Thomas, O.R.T. and Overton, T.W. (2017) Flow Cytometry as a Rapid Analytical Tool to Determine Physiological Responses to Changing O_2 and Iron Concentration by *Magnetospirillum gryphiswaldense* Strain MSR-1. *Scientific Reports*, **7**, Article No. 13118. https://doi.org/10.1038/s41598-017-13414-z

[39] Bína, D., Herbstová, M., Gardian, Z., Vácha, F. and Litvín, R. (2016) Novel Structural Aspect of the Diatom Thylakoid Membrane: Lateral Segregation of Photosystem I under Red-Enhanced Illumination. *Scientific Reports*, **6**, Article No. 25583. https://doi.org/10.1038/srep25583

[40] Leyland, B., Boussiba, S. and Khozin-Goldberg, I. (2020) A Review of Diatom Lipid Droplets. *Biology* (*Basel*), **9**, E38. https://doi.org/10.3390/biology9020038

[41] Yang, R. and Wei, D. (2020) Improving Fucoxanthin Production in Mixotrophic Culture of Marine Diatom *Phaeodactylum tricornutum* by LED Light Shift and Nitrogen Supplementation. *Frontiers in Bioengineering and Biotechnology*, **8**, 820. https://doi.org/10.3389/fbioe.2020.00820

[42] Gaytán-Luna, D.E., Ochoa-Alfaro, A.E., Rocha-Uribe, A., Pérez-Martínez, A.S., Alpuche-Solís, Á.G. and Soria-Guerra, R.E. (2016) Effect of Green and Red Light in Lipid Accumulation and Transcriptional Profile of Genes Implicated in Lipid Biosynthesis in *Chlamydomonas reinhardtii*. *Biotechnology Progress*, **32**, 1404-1411. https://doi.org/10.1002/btpr.2368

[43] Severes, A., Hegde, S., D'Souza, L. and Hegde, S. (2017) Use of Light Emitting Diodes (LEDs) for Enhanced Lipid Production in Micro-Algae Based Biofuels. *Journal of Photochemistry and Photobiology B*: *Biology*, **170**, 235-240. https://doi.org/10.1016/j.jphotobiol.2017.04.023

[44] Heydarizadeh, P., Veidl, B., Huang, B., Lukomska, E., Wielgosz-Collin, G., Couzinet-Mossion, A., Bougaran, G., Marchand, J. and Schoefs, B. (2019) Carbon Orientation in the Diatom *Phaeodactylum tricornutum*: The Effects of Carbon Limitation and Photon Flux Density. *Frontiers in Plant Science*, **10**, 471. https://doi.org/10.3389/fpls.2019.00471

[45] Li, Y., Xu, J. and Gao, K. (2014) Light-Modulated Responses of Growth and Photosynthetic Performance to Ocean Acidification in the Model Diatom *Phaeodactylum tricornutum*. *PLOS ONE*, **9**, e96173. https://doi.org/10.1371/journal.pone.0096173

[46] Molino, J.V.D., de Carvalho, J.C.M. and Mayfield, S. (2018) Evaluation of Secretion Reporters to Microalgae Biotechnology: Blue to Red Fluorescent Proteins. *Algal Research*, **31**, 252-261. https://doi.org/10.1016/j.algal.2018.02.018

[47] Braun-Galleani, S., Baganz, F. and Purton, S. (2015) Improving Recombinant Protein Production in the *Chlamydomonas reinhardtii* Chloroplast Using Vivid Verde Fluorescent Protein as a Reporter. *Biotechnology Journal*, **10**, 1289-1297. https://doi.org/10.1002/biot.201400566

[48] Fabris, M., George, J., Kuzhiumparambil, U., Lawson, C.A., Jaramillo-Madrid, A.C., Abbriano, R.M., Vickers, C.E. and Ralph (2020) Extrachromosomal Genetic Engineering of the Marine Diatom *Phaeodactylum tricornutum* Enables the Heterologous Production of Monoterpenoids. *ACS Synthetic Biology*, **9**, 598-612. https://doi.org/10.1021/acssynbio.9b00455

[49] Kuczynska, P., Jemiola-Rzeminska, M. and Strzalka, K. (2015) Photosynthetic Pigments in Diatoms. *Marine Drugs*, **13**, 5847-5881. https://doi.org/10.3390/md13095847

[50] Morikawa, T.J., Fujita, H., Kitamura, A., Horio, T., Yamamoto, J., Kinjo, M., Sasaki, A., Machiyama, H., Yoshizawa, K., Ichimura, T., Imada, K., Nagai, T. and Watanabe, T.M. (2016) Dependence of Fluorescent Protein Brightness on Protein Concentration in Solution and Enhancement of It. *Scientific Reports*, **6**, Article No. 22342. https://doi.org/10.1038/srep22342

[51] Myšková, J., Rybakova, O., Brynda, J., Khoroshyy, P., Bondar, A. and Lazar, J. (2020) Directionality of Light Absorption and Emission in Representative Fluorescent Proteins. *Proceedings of the National Academy of Sciences*, **117**, 32395-32401. https://doi.org/10.1073/pnas.2017379117

[52] Barstow, B., Ando, N., Kim, C.U. and Gruner, S.M. (2009) Coupling of Pressure-Induced Structural Shifts to Spectral Changes in a Yellow Fluorescent Protein. *Biophysical Journal*, **97**, 1719-1727. https://doi.org/10.1016/j.bpj.2009.06.039

[53] Bai, X., Song, H., Lavoie, M., Zhu, K., Su, Y., Ye, H., Chen, S., Fu, Z. and Qian, H. (2016) Proteomic Analyses Bring New Insights into the Effect of a Dark Stress on Lipid Biosynthesis in *Phaeodactylum tricornutum*. *Scientific Reports*, **6**, Article No. 25494. https://doi.org/10.1038/srep25494

[54] Jayakumar, S., Bhuyar, P., Pugazhendhi, A., Rahim, M.H.A., Maniam, G.P. and Govindan, N. (2021) Effects of Light Intensity and Nutrients on the Lipid Content of Marine Microalga (diatom) Amphiprora sp. for Promising Biodiesel Production. *Science of the Total Environment*, **768**, Article ID: 145471. https://doi.org/10.1016/j.scitotenv.2021.145471

[55] Yang, Z.-K., Niu, Y.-F., Ma, Y.-H., Xue, J., Zhang, M.-H., Yang, W.-D., Liu, J.-S.,

Lu, S.-H., Guan, Y. and Li, H.-Y. (2013) Molecular and Cellular Mechanisms of Neutral Lipid Accumulation in Diatom Following Nitrogen Deprivation. *Biotechnology for Biofuels*, **6**, 67. https://doi.org/10.1186/1754-6834-6-67

[56] Abida, H., Dolch, L.-J., Meï, C., Villanova, V., Conte, M., Block, M.A., Finazzi, G., Bastien, O., Tirichine, L., Bowler, C., Rébeillé, F., Petroutsos, D., Jouhet, J. and Maréchal, E. (2014) Membrane Glycerolipid Remodeling Triggered by Nitrogen and Phosphorus Starvation in *Phaeodactylum tricornutum. Plant Physiology*, **167**, 118-136. https://doi.org/10.1104/pp.114.252395

[57] Kobayashi, K., Endo, K. and Wada, H. (2016) Roles of Lipids in Photosynthesis. *Subcellular Biochemistry*, **86**, 21-49. https://doi.org/10.1007/978-3-319-25979-6_2

[58] Valentine, R.C. and Valentine, D.L. (2004) Omega-3 Fatty Acids in Cellular Membranes: A Unified Concept. *Progress in Lipid Research*, **43**, 383-402. https://doi.org/10.1016/j.plipres.2004.05.004

[59] Duarte, B., Feijão, E., Goessling, J.W., Caçador, I. and Matos, A.R. (2021) Pigment and Fatty Acid Production under Different Light Qualities in the Diatom *Phaeodactylum tricornutum. Applied Sciences*, **11**, 2550. https://doi.org/10.3390/app11062550